How Long Do Regions of Different Dynamics Persist in Supercooled *o*-Terphenyl?

Chia-Ying Wang and M. D. Ediger*

Department of Chemistry, University of Wisconsin-Madison, 1101 University Avenue, Madison, Wisconsin 53706

Received: October 23, 1998; In Final Form: December 31, 1998

In supercooled *o*-terphenyl (OTP), subsets of probe molecules in more mobile environments can be selectively photobleached. The time required for the remaining slower-than-average probes to be redistributed into an equilibrium set of environments has been measured. At $T_g + 4$ K ($T_g = 243$ K), this exchange time is 6 times greater than the average probe rotational correlation time. These results are compared to previous optical measurements at $T_g + 1$ K (Cicerone, M. T.; Ediger, M. D. *J. Chem. Phys.* **1995**, *103*, 5684), which showed that the exchange time is more than 100 times the rotational correlation time, and to multidimensional NMR experiments on deuterated OTP at $T_g + 10$ K (Bohmer, R.; et al. *Europhys. Lett.* **1996**, *36*, 55), which showed that the exchange time is nearly equal to the correlation time. These results in aggregate suggest that a new relaxation process in equilibrium supercooled liquids emerges only at temperatures very near T_g. A model for selective photobleaching is proposed. The model reproduces the experimental data reasonably well and indicates that the photobleaching efficiency of a given probe is only weakly correlated with its rotational correlation time.

I. Introduction

The fundamental origin of the characteristic nonexponential relaxation processes in supercooled liquids and amorphous polymers has been in dispute for decades. Interest in this issue was revived recently as new experimental techniques have been developed to provide more explicit investigations.[1−7] Nonexponential relaxation can be interpreted in two fundamentally different ways. One possibility is that a heterogeneous set of environments exists in supercooled liquids; relaxation within a single environment is essentially exponential, but the relaxation time varies significantly among environments. Alternatively, environments are homogeneous in supercooled liquids and each molecule relaxes nearly identically in an intrinsically nonexponential manner. Most recent experiments indicate that the heterogeneous explanation is more nearly correct,[2−7] although this view is not unanimous.[8] The size of heterogeneous dynamic regions is estimated to be 2−3 nm,[9−11] and the width of the distribution of relaxation times is proposed to be 2−3 orders of magnitude.[9,12] However, this heterogeneity cannot last forever; i.e., exchange must occur between domains of different dynamics since supercooled liquids are ergodic. Is this exchange time much longer than or comparable to the ensemble-averaged relaxation time? We will focus on the issue of the lifetime of the heterogeneous dynamic regions in this report.

Spiess and co-workers[13,14] first measured the lifetime of the heterogeneous dynamic domains in polymeric glass formers using a reduced four-dimensional NMR experiment which selectively observed a slow subensemble of C−H vectors. In studies on poly(vinyl acetate), they observed that the slow subensemble gradually became an average subensemble on a time scale which we can identify as the exchange time. At $T_g + 20$ K, the exchange time was twice the average relaxation time of a C−H vector. These observations demonstrated that poly(vinyl acetate) exhibits a heterogeneous distribution of relaxation times above T_g and that this heterogeneity possesses a lifetime comparable to the ensemble-averaged relaxation time. Recently, similar observations for another polymeric glass former, polystyrene, were reported by the same group.[15] At $T_g + 10$ K, the exchange time is comparable to the average relaxation time of polymer segments.

For low molecular weight glass formers, Cicerone and Ediger first reported direct observation of spatially heterogeneous dynamics. They used a photobleaching technique to measure probe reorientation times in supercooled *o*-terphenyl (OTP).[4] Cicerone and Ediger were able to selectively photobleach probe molecules in more mobile environments and observe the dynamics of the remaining probes. With time, the environments of these remaining probe molecules evolve into an equilibrium set of environments. At $T_g + 1$ K, an exceedingly long time is required to realize this reequilibration; some initially "slow" environments remain slow even after the molecules in these environments have reoriented more than 100 times. Since the probe, tetracene, and the OTP host molecules have similar rotational behavior,[16] it is expected that similarly long exchange times exist for OTP molecules at $T_g + 1$ K.

Soon thereafter, Bohmer et al. reported multidimensional NMR experiments on deuterated OTP at $T_g + 10$ K.[2] They found that the characteristic time scales for molecular reorientation and dynamic exchange are similar in supercooled OTP. This conclusion seems inconsistent with the results of the photobleaching experiments described in the previous paragraph. However, there is a temperature difference of nearly 10 K between the optical measurements and the NMR experiments. Could the exchange time exhibit such a strong temperature dependence?

Here we report experiments which explore the effect of temperature on the lifetimes of heterogeneous dynamic domains in supercooled liquids. We performed photobleaching experiments analogous to those reported in ref 4 on tetracene in OTP at $T_g + 4$ K. Strikingly, the exchange time is determined to be 6.5 times the average probe correlation time at $T_g + 4$ K whereas the exchange time is 540 times slower than the probe reorienta-

10.1021/jp984149x CCC: $18.00
Published on Web 02/19/1999

tion at $T_g + 1$ K. These results allow a consistent interpretation with NMR measurements at $T_g + 10$ K and suggest that a new relaxation process may emerge in supercooled liquids only at temperatures very near T_g.

To develop a more quantitative understanding of the photobleaching selectivity, we introduce a model for the photobleaching experiments. The model reasonably reproduces the experimental data for tetracene in OTP at $T_g + 4$ K and suggests a weak photobleaching selectivity among probes in different dynamic environments.

II. Experimental Section

A complete description of the photobleaching technique and method of sample preparation can be found in reference 16. Here we briefly review this technique since some details are pertinent to the interpretation and discussion of results presented in this paper.

A. Standard Photobleaching. Many different probe molecules may be photobleached with intense visible light to yield photoproducts which do not absorb visible wavelengths. When a probe molecule with a strongly polarized electronic transition is photobleached with a linearly polarized writing beam, an orientational anisotropy in the probe population is created. A weak reading beam whose polarization is either parallel or perpendicular to the polarization of the writing beam can probe this orientational anisotropy. With time, the unbleached probe molecules reorient and reach an isotropic distribution. As a result, the difference between the parallel and perpendicular fluorescence intensities decreases and eventually becomes zero. This fluorescence modulation decay defines the anisotropy $r(t)$ of the probe orientational distribution. *Only the reorientation of unbleached probe molecules is observed in the photobleaching experiment*; bleached probes do not absorb the reading beam and thus do not contribute to the fluorescence signal. The bleach depth, the fraction of probe molecules which have been bleached, is ≤ 0.1 in the standard photobleaching experiment. When the bleach depth is this small, the acquired anisotropy function describes essentially the entire ensemble of probes. Figure 1a schematically illustrates the write/read sequences used in the standard-photobleaching experiment.

The probe rotational correlation function, CF(t), is defined in terms of the anisotropy:

$$\mathrm{CF}(t) \equiv r(t)/r(0) \tag{1}$$

where $r(0)$ is the extrapolation of $r(t)$ to time zero. Typically, the rotational correlation function decays nonexponentially and is usually fit with the Kohlrausch−Williams−Watts (KWW) function:

$$\mathrm{CF}(t) \approx e^{-(t/\tau_{\mathrm{KWW}})^{\beta}} \tag{2}$$

A model-independent rotational correlation time, τ_c, is defined as the integral of the correlation function and can be calculated from the KWW fitting result:

$$\tau_c \equiv \int_0^{\infty} \mathrm{CF}(t)\, \mathrm{d}t = \frac{\tau_{\mathrm{KWW}}}{\beta}\Gamma\left(\frac{1}{\beta}\right) \tag{3}$$

B. Deep Photobleaching: Varying Bleach Depth. With an increase in the bleaching time, a larger fraction of the probe molecules are photobleached. In the deep-photobleaching experiment, an intense linearly polarized writing beam is used to produce bleach depths >0.1 (see Figure 1b). The rotational correlation time of the remaining probe molecules, τ_{obs}, is then determined via the measurements of the fluorescence intensities from a weak modulated reading beam, following the same procedure as the standard-photobleaching experiment (eqs 1−eq 3).

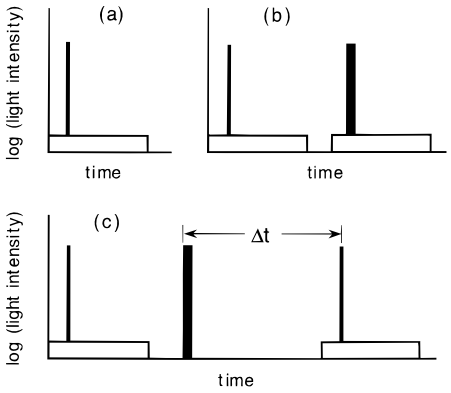

Figure 1. Schematic representation of write/read sequences for photobleaching experiments. In each part of the figure, the high-intensity light represents the bleaching beams and the low-intensity light represents the reading beams. (a) Standard photobleaching. The sample is bleached 10%, and τ_c is determined. (b) Deep photobleaching with varying bleach depth. First, a standard-photobleaching experiment is performed to obtain τ_c. Then, on the same spot, the sample is bleached $>10\%$ with longer bleaching time to obtain τ_{obs}. (c) Deep photobleaching with varying time. After the equilibrium correlation time, τ_c is determined from a standard-photobleaching experiment, the sample is bleached 65%, creating a nonequilibrium distribution of unbleached probe mobilities. After a waiting time Δt, the sample is bleached again at 10% to obtain $\tau_{obs}(\Delta t)$. The entire procedure is performed on a single spot in the sample.

Previously Cicerone and Ediger reported that the rotational correlation time τ_{obs} observed after a deep bleach is longer than the correlation time τ_c obtained from the standard-photobleaching experiment for tetracene in OTP at $T_g + 1$ K.[4] They suggested that a distribution of probe mobilities exists and that the observation of longer rotation times after a deep bleach can be explained by the selective destruction of probes in more mobile environments.

How is this selective photobleaching to be understood? The photobleaching reaction of tetracene with oxygen likely changes the planar tetracene molecule into a nonplanar peroxide.[17] More mobile environments may result from lower-than-average local matrix densities, and probe molecules in these environments may be more likely to undergo the conformational change required for photoreaction. Figure 2 illustrates this possibility schematically with small circles representing matrix molecules, rectangles representing unbleached probe molecules, and the black distorted shapes representing photobleached probes. In region a, lower density results in higher photobleaching efficiency whereas in region b, higher density results in lower photobleaching efficiency. Since it is likely that the mobility is higher in regions of low density, this scenario predicts a tendency toward selective bleaching of more mobile probes. The above description is one of several possible explanations for selective photobleaching. Another possibility is that the diffusion of oxygen molecules (needed for photobleaching) is enhanced in the more mobile environments.

C. Deep Photobleaching: Varying Time. After a deep bleach, the remaining slower-than-average probes will reestablish the equilibrium distribution through exchange between regions of different dynamics. That is, the observed correlation time τ_{obs} immediately after a deep bleach is longer than the equilibrium correlation time τ_c and gradually decays toward τ_c as the remaining probes are redistributed into an equilibrium set of environments.

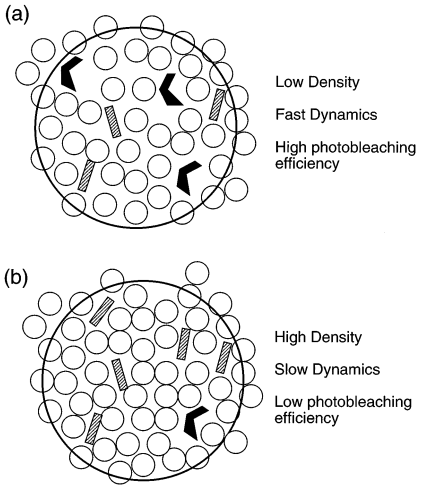

Figure 2. Schematic illustration of different photobleaching efficiencies in regions of different local densities. Small circles represent matrix molecules, and the rectangles are unbleached probe molecules. The black distorted shapes represent photobleached probes. In region a, lower density results in higher photobleaching efficiency since the probe is more likely to be able to make the change in conformation required by photobleaching. In region b, higher density results in lower photobleaching efficiency.

The time scale for the above process is the exchange time τ_{ex} and can be determined via the following procedure (see Figure 1c). First, we measure the equilibrium correlation time τ_c using the standard-photobleaching technique (reading after a shallow bleach with bleach depth ≤ 0.1). Second, a deep bleach (bleach depth ≈ 0.65) at the same spot of the sample is performed with circularly polarized light. Circularly polarized light is used to avoid any orientational anisotropy induced by this deep bleach. Third, after a waiting time Δt, another shallow bleach with linear polarization is performed at the same spot to create the orientational anisotropy. The fluorescence modulation is then measured in order to determine the rotational correlation time τ_{obs} at time Δt. By varying Δt, the time evolution of τ_{obs} is obtained and the exchange time between regions of different dynamics can be determined.

All of these experiments were performed on well-equilibrated samples of OTP. Typically, samples were held at constant temperature for 1 day before beginning measurements. Standard-photobleaching experiments yielded the same rotational correlation times whether the samples had been held isothermally for 1 day or 2 weeks. $T_g = 243$ K is the onset of the glass transition, determined by differential scanning calorimetry (10 K/min).

Samples with optical densities ranging from 0.4 to 0.7 were held in a 5 mm cuvette, and 100 mW/mm^2 of 476-nm light from a continuous-wave Ar^+ laser was used to photobleach tetracene, with the duration of the bleaching pulse being 0.1−0.2 s for the 10% linearly polarized shallow bleach. For tetracene in supercooled OTP at $T_g + 4$ K, the equilibrium correlation time τ_c was measured to be 13 s and the bleaching time for the 65% deep bleach ranged from 1 to 1.5 s. At $T_g + 1$ K, τ_c was 125 s and the bleaching time for the 65% deep bleach ranged from 2 to 6 s. At both temperatures, the initial anisotropy $r(0)$ obtained for the shallow-bleaching experiments was about 0.2 irrespective of whether the shallow bleach preceded or followed the deep bleach. For the deep-bleaching experiments, typically seven experiments were performed at each Δt to improve precision.

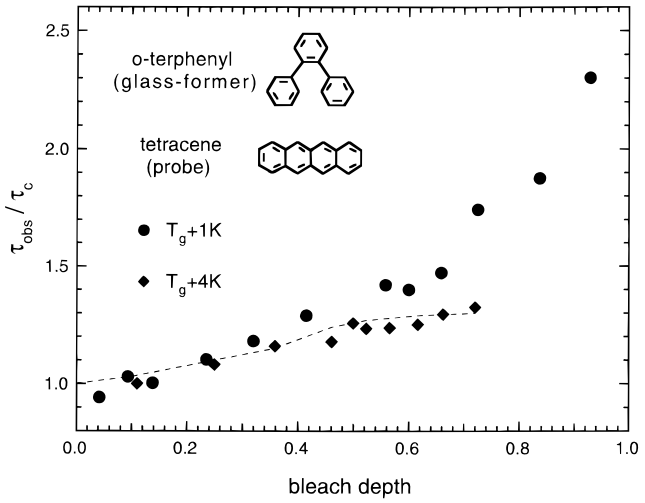

Figure 3. Values of observed correlation times (τ_{obs}) measured immediately following a bleach as a function of bleach depth. These values have been divided by those obtained in the limit of a shallow bleach (τ_c). Solid circle = 244 K ($T_g + 1$ K)[4] and solid diamond = 247 K ($T_g + 4$ K) for tetracene in OTP. The dashed line is the model result for $T_g + 4$ K discussed in section IV.

TABLE 1: KWW β Parameters for Tetracene in OTP at 247 K ($T_g + 4$ K) and 244 K ($T_g + 1$ K)

exptl method	temp, (K)	β(exptl fit)	β(model)[a]
shallow bleach	247	0.62 ± 0.02	0.59
	244	0.62 ± 0.02	
65% deep bleach	247	0.67 ± 0.03	0.66
	244	0.69 ± 0.03	
shallow bleach following a 65% deep bleach	247	0.60 ± 0.03	0.64
	244	0.59 ± 0.02	

[a] These values of β are calculated from the model (section IV). The input β for the model is 0.6.

III. Results and Discussion

This section presents photobleaching results for tetracene in OTP. We reiterate that we expect the dynamics of OTP molecules to be very similar to what is observed for tetracene, on the basis of the similarity between their rotation behavior.[16]

A. τ_{obs} vs Bleach Depth. Figure 3 displays the ratio τ_{obs}/τ_c as a function of bleach depth for tetracene in OTP at $T_g + 1$ K[4] and $T_g + 4$ K. Values of τ_{obs} represent the average rotation time of the probes which remain after the indicated fraction of the probe molecules have been destroyed by photobleaching (experimental method described in section IIB). For both temperatures, probe reorientation becomes significantly slower as bleach depth is increased. As discussed above in connection with Figure 2, we are able to selectively bleach probe molecules in more mobile environments and observe the dynamics of those probes which remain in slower subensembles. However, the selectivity of photobleaching is decreased with increasing temperature. As shown in Figure 3, the bleach depth dependence of τ_{obs}/τ_c at $T_g + 4$ K is not as strong as that at $T_g + 1$ K.

Table 1 lists the KWW β parameters obtained from fitting the experimental data and from calculations using the model discussed in section IV. For those values of β obtained after a shallow bleaching following the 65% deep bleach, no trend was observed for different waiting times Δt. Consequently, only the average of the fitting results over all waiting times is reported.

B. Exchange Time. The observation that the average probe rotation time τ_{obs} increases as a function of bleach depth demonstrates that a nonequilibrium distribution of reorientation

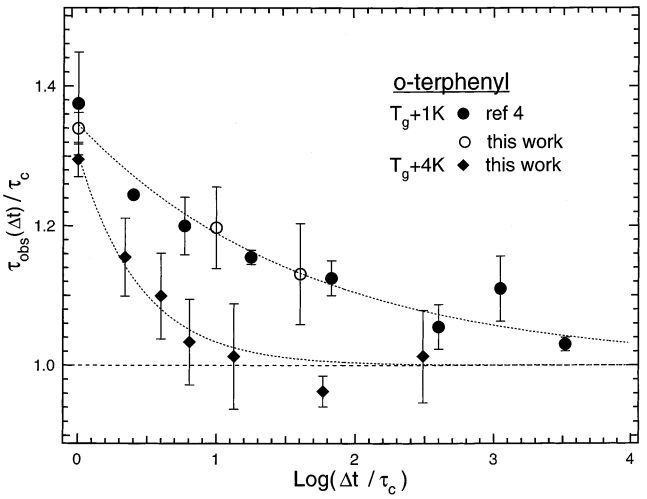

Figure 4. $\tau_{obs}(\Delta t)$ as a function of the delay time Δt after a 65% deep bleach for tetracene in OTP at $T_g + 1$ K (solid circle)[4] and $T_g + 4$ K (solid diamond). The dotted lines are fits used for calculating the exchange time, i.e., the time required for a slow subset of probes to become an average subset. Open circles at $T_g + 1$ K represent new measurements and confirm the reliability of the original measurements.

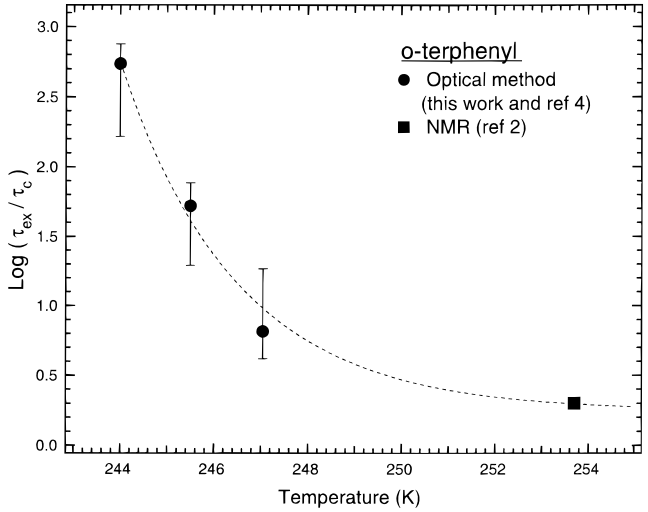

Figure 5. Temperature dependence of the exchange time (τ_{ex}) divided by the rotational correlation time (τ_c). Even after normalization to τ_c, the time required for a molecule to change dynamic environments is a strong function of temperature near T_g.

times within the probe molecule population is created by a deep bleach. Eventually, the remaining probes will be redistributed into a random set of environments because of exchange between regions of different dynamics. Thus the values of τ_{obs} should tend toward their equilibrium value τ_c as time increases following the initial deep bleach. This experiment does not establish the mechanism by which exchange occurs. Exchange could be due to a fluctuation in the dynamic character of a region, the translational diffusion of a probe out of a region with particular dynamic characteristics, or a process which couples these two.

After a deep bleach (bleach depth ≈ 0.65), $\tau_{obs}(\Delta t)$ was measured with various waiting times Δt for tetracene in OTP at $T_g + 4$ K by following the method described in section IIC. The results are displayed in Figure 4 with a log time scale. The time evolution of $\tau_{obs}(\Delta t)$ results from the exchange between regions of different dynamics. Hence, the exchange time is defined and can be calculated by integration of the area under $[\tau_{obs}(\Delta t)/\tau_c - 1]/[\tau_{obs}(\Delta t = 0)/\tau_c - 1]$. As shown in Figure 4, an exponential function (in log time) fits the $\tau_{obs}(\Delta t)$ data reasonably well. The exchange time is then calculated by integrating the fit function with the maximum waiting time as a long time cutoff. An exchange time of $6.5\tau_c$ is obtained for tetracene in OTP at $T_g + 4$ K. Data at $T_g + 1$ K obtained by Cicerone and Ediger[4] is also plotted in Figure 4, and the exchange time is calculated as $540\tau_c$ by employing the same approach. Some measurements were repeated at $T_g + 1$ K (shown as open circles in Figure 4), and these new results are consistent with the results reported by Cicerone and Ediger[4] even though different excitation wavelengths were used (476 nm for the new measurements vs 488 nm previously).

At $T_g + 1$ K, the dynamics of the slower environments in which the probes initially reside have not completely randomized even after these probes and the surrounding OTP molecules have reoriented more than 100 times. Strikingly, only 3 K higher, the environments reach equilibrium after probe and host molecules reorient roughly 6 times!

Since tetracene molecules and OTP molecules exhibit similar rotational characteristics in OTP over a wide temperature range,[16] we assume that the probe rotational dynamics observed in these deep-bleaching experiments reasonably represents the matrix dynamics and can be compared to measurements on OTP. Figure 5 displays the temperature dependence of the exchange time obtained from optical experiments at $T_g + 1$ K,[4] $T_g + 2.5$ K, and $T_g + 4$ K. The exchange time at $T_g + 2.5$ K was estimated from measurements of $\tau_{obs}(\Delta t)$ for tetracene in OTP at few waiting times employing the method described in section IIIB. Also shown in Figure 5 are NMR results at $T_g + 10$ K from Sillescu and co-workers.[2] To interpret the multidimensional NMR experiments, a dimensionless rate memory parameter Q[18] was introduced as the ratio of slow relaxation rates to the exchange rate between slow and fast regions. For deuterated OTP, Sillescu and co-workers fit the experimental data at $T_g + 10$ K with the minimal rate memory ($Q = 1$). We interpret this as indicating that the exchange time τ_{ex} and the correlation time τ_c are very nearly equal. While experimental results are not available for OTP for temperatures greater than $T_g + 10$ K, it is likely that $\log(\tau_{ex}/\tau_c)$ continues to be ≈ 0 up to much higher temperatures.

Figure 5 illustrates that the photobleaching results very near T_g can be fully reconciled with the NMR results at $T_g + 10$ K. The results indicate that an extremely slow relaxation process emerges in supercooled OTP as the temperature is lowered to very near T_g. This striking result was obtained from experiments performed on samples in the *equilibrium* supercooled state. Thus, the emerging slow relaxation process cannot be associated in any way with the kinetic aspects of the laboratory glass transition. This new time scale might imply that a thermodynamic singularity is nearby. Many theories of the glass transition are based on a thermodynamic singularity somewhat below the laboratory T_g,[19−24] but the experimental evidence (i.e., the emergence of a new time scale or length scale as the temperature is lowered) for such a singularity has been quite indirect.

As a test of the generality of this phenomenon among glass-forming materials, similar photobleaching experiments are being performed on a polymeric glass former, polystyrene. Preliminary results indicate that the exchange time (as probed by tetracene reorientation) is substantially longer than the α-relaxation time. Thus these preliminary results on polystyrene are consistent with the results reported here for OTP.

C. Comparison with Work on Other Glass-Formers. Is the new relaxation process implied by Figure 5 consistent with

experiments on other materials? Recently, MacPhail and co-workers also observed an ultraslow relaxation process in their studies of nonequilibrium dynamics in supercooled glycerol by stimulated Brillouin gain spectroscopy.[25] These authors argued that this ultraslow process could result either from the heterogeneous nature of dynamics in supercooled liquids or from the relaxation of mechanical strain built up in the sample during the measurements.

Schiener et al. successfully performed dielectric hole-burning experiments of propylene carbonate and glycerol near their glass transitions.[3] This observation provides evidence for the existence of a distribution of relaxation times in these supercooled liquids. The observed time scale for hole refilling is very similar to that characterizing the α-relaxation at temperatures close to T_g. Although this result has sometimes been interpreted as indicating that the exchange time is equal to the α-relaxation time, we support this view expressed in ref 3: "The present finding of a reequilibration time scale of the order of the α-relaxation time does therefore not necessarily imply that the exchange among different parts of the relaxation time spectrum also occur relatively fast." If the exchange time were equal to the α-relaxation time, hole broadening would be observed as the hole fills. Since this is not observed, we interpret these dielectric results as indicating that the exchange time is longer than the α-relaxation time and could be much longer.

Very recently, Russell et al. investigated thermal fluctuations in the dielectric properties of a poly(vinyl acetate) film near a scanning probe tip.[6] Anomalous variations in the noise spectrum were interpreted as arising from fluctuations in the relaxation time spectrum of a 50 nm volume of the film at the surface. These authors modeled their results with a correlation size of 10 nm and heterogeneity lifetimes roughly comparable to the α-relaxation time. Since these experiments were performed near and below the usually reported T_g for poly(vinyl acetate), they address the same temperature range as the measurements reported here. The apparent difference in the conclusions regarding the heterogeneity lifetimes certainly invites further investigation and might be attributed to the different glass-formers used. Experiments on OTP with the nanoscale dielectric fluctuation technique would be particularly interesting.

A number of simulation studies recently showed evidence for spatially heterogeneous dynamics in supercooled liquids.[26−28] In cases where the heterogeneity lifetimes were investigated, it was found that exchange times are roughly comparable to the α-relaxation times. Since these simulations represent systems far above the laboratory glass transition, these results should be viewed as consistent with the results presented here. On the other hand, recent calculations by Spiess and co-workers using a lattice model glass suggest the exchange time between regions of heterogeneous dynamics has a weak temperature dependence.[29] This result is difficult to reconcile with the current observations.

D. Possible Artifacts. Since the results shown in Figure 5 are so striking, we have spent considerable effort investigating whether these experiments are reproducible and whether any artifact might be influencing our interpretation. We are confident that the results are reproducible and show evidence in Figure 4 that different experimentalists using different samples produce the same results within the reported error bars. It is impossible to be completely confident that no artifact is influencing the interpretation of these (or any other) experiments. Cicerone and Ediger considered some possible artifacts and argued that the observed heterogeneous domains are not induced by the probes and are not the result of local heating.[4] Here we consider three additional possible artifacts. Our conclusion is that none of these potential artifacts provide an alternate interpretation for the data in Figure 4.

Do tetracene dimers play a role in the deep photobleaching experiment? Angell and co-workers reported that the equilibration times for a probe monomer−dimer equilibrium in sorbitol at temperatures near T_g were 10^4-10^5 times longer than the matrix shear relaxation times.[30] One might wonder if the extraordinarily long decay of $\tau_{obs}(\Delta t)$ at $T_g + 1$ K is due to the tetracene monomer−dimer reequilibration. For this to be the case, a mixture of monomers and dimers would need to exist at equilibrium and the monomers would need to be selectively photobleached. In this scenario, the longer τ_{obs} would be attributed to the remaining slower dimer molecules. Two investigations were performed to test this possibility, both based on the observation that tetracene dimers have an absorption spectrum distinctly different from that of tetracene monomers in the range of wavelengths used to perform the deep-photobleaching experiment.[31] First, the absorption spectrum of tetracene in OTP under the conditions of these experiments did not show any evidence of dimer formation. Second, since the dimer spectrum is quite different, using different excitation wavelengths would change the ratio of dimer/monomer photobleached and thus different values of the average correlation time τ_{obs} would be obtained. Nevertheless, as shown in Figure 4, measurements at $T_g + 1$ K using two different excitation wavelengths yielded consistent results. Consequently, it is implausible to presume that the evolution of $\tau_{obs}(\Delta t)$ results from probe monomer−dimer reequilibration.

Does volume relaxation of the matrix influence the measurements of the probe correlation times? During a deep bleach, most probes are converted to a different chemical species, the photoproduct. We then examined the rotational behavior of the unbleached probes at various times. On average, each unbleached probe is about 25 nm from the nearest bleached probe. Could a molecular volume change associated with photobleaching induce an internal pressure in the sample which would modify the behavior of the unbleached species? A simple calculation of the effect indicates that the resulting ΔP is less than 0.15 bar and that the associated change in relaxation time, $\Delta\tau/\tau$, is less than 0.003. This calculation indicates that this effect is 2 orders of magnitude too small to account for the experimental observation. As a check, we measured the volume relaxation at $T_g + 1$ K by monitoring the equilibration of the probe dynamics after a temperature jump from 3 K higher. The observed probe correlation time reached its equilibrium value τ_c by a waiting time of $50\tau_c$ after the temperature jump.[32] In contrast, in the deep-photobleaching experiments shown in Figure 4, $\tau_{obs}(\Delta t)$ is still significantly slower than τ_c at the $50\tau_c$ waiting time at the same temperature $T_g + 1$ K. Thus we conclude that the photobleaching of some probe molecules is unlikely to influence the dynamics of the remaining probes.

Could oxygen diffusion play a role in the deep photobleaching experiment? Conceivably oxygen might be depleted in some regions of the sample as a result of the deep bleach. Assuming an oxygen diffusion coefficient of 10^{-10} cm^2/s, reequilibration on the length scale of 3 nm would occur in 10^{-4} s. Clearly, oxygen diffusion is too fast to be responsible for the very slow exchange times observed here.

None of these considerations to our knowledge contribute to the observed relaxation of the probe correlation time $\tau_{obs}(\Delta t)$ after a deep bleach or influence our interpretation of Figure 4.

IV. Model of Selective Bleaching

To develop a more quantitative understanding of the selectivity of photobleaching, we introduce a model to simulate the bleach-depth dependence of tetracene rotational correlation times in OTP at $T_g + 4$ K (shown in Figure 3). The results reasonably reproduce the experimental data and suggest that the photobleaching efficiency of a given probe is only weakly correlated with its rotational correlation time.

A. Model Assumptions. The following assumptions are made to construct the model: (i) there is a distribution of regions with different dynamics; (ii) relaxation is exponential within a region; (iii) dynamic heterogeneity is static on the time scale of reorientation (i.e., no exchange occurs among regions of heterogeneous dynamics); (iv) the dynamics and photophysical behavior of one set of probes are not influenced by bleaching another set; (v) all regions are equally illuminated during the bleaching period; and (vi) photobleaching efficiency only depends on the mobility of the environments where probe molecules reside, i.e. the probe reorientation time in a given region.

On the basis of the above assumptions, the bleach depth (bd_i) for regions with probe rotational correlation time τ can be expressed as a function of $\Phi(\tau)$, where $\Phi(\tau)$ is the photobleaching efficiency function. For convenience, the photobleaching efficiency function is chosen to be a power law of the probe correlation time τ:

$$\Phi(\tau) \propto 1/\tau^{\alpha} \tag{4}$$

If $\alpha = 0$, bleaching is not selective. If $\alpha > 0$, probe molecules in more mobile environments are being bleached more effectively.

The equilibrium distribution of probe rotation times is taken to be given by a KWW distribution function $g(\tau)$ with the KWW parameter β equal to 0.6.[33,34] The bleach depth of the whole ensemble is then calculated using the weighted summation of the bleach depths from regions of different dynamics:

$$\text{bleach depth} = \frac{\sum_i g_i(\text{bd}_i)}{\sum_i g_i} = \frac{\sum_\tau g(\tau)\, f(\Phi(\tau))}{\sum_\tau g(\tau)} \tag{5}$$

The Appendix presents details for the calculation of the bleach depth and the rotational correlation time from the remaining distribution of unbleached probes.

Probe reorientation during the bleaching period is considered in order to model more closely the actual photobleaching experiments. Subsets of probe molecules with rotational correlation times much shorter than the bleaching time reorient and approach an isotropic distribution of orientations during the bleaching period and thus make no contribution to the anisotropy measurement. Furthermore, the photobleaching efficiency is enhanced in those regions where probe molecules partially or completely reorient during the bleaching duration. These two effects are included in an approximate manner in the model, which uses the experimental bleaching time as an input (see Appendix).

B. Model Solution. We start with an initial guess of the power α in the photobleaching efficiency function $\Phi(\tau)$. τ_{obs} is calculated as a function of bleach depth. The equilibrium rotational correlation time τ_c is obtained for a bleach depth near zero, e.g., 0.01. The value of α is iterated until the calculated results for bleach depth dependence of τ_{obs}/τ_c match the experimental data (Figure 3) as well as possible.

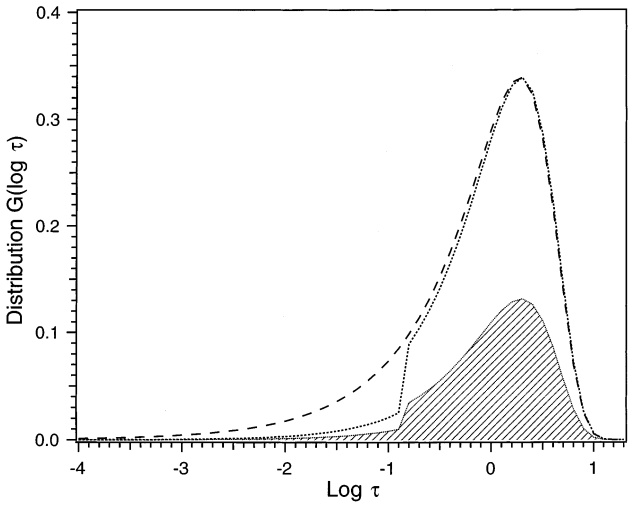

Figure 6. Distributions of probe relaxation times. The dashed curve represents the equilibrium KWW distribution with $\beta = 0.6$. The shadowed area represents the distribution remaining after a 65% deep bleach with the photobleaching efficiency function $\Phi(\tau) \propto 1/\tau^{0.08}$. The dotted curve shows this postbleach distribution normalized to the peak of the original distribution. The postbleach distribution differs from the original distribution both because of the photobleaching efficiency function and because of the fact that molecules which can reorient during bleaching are more efficiently bleached.

C. Model Results. *(a) Bleaching Selectivity.* The dashed line in Figure 3 displays results with $\alpha = 0.08$. This choice reproduces the observed bleach-depth dependence of the average probe rotational correlation time τ_{obs}. The photobleaching efficiency function $\Phi(\tau) \propto 1/\tau^{0.08}$ indicates a weak photobleach selectivity among probes in heterogeneous dynamic domains. In addition, for those probes with correlation times shorter than the bleaching time, bleaching is even more efficient, as discussed above. Figure 6 illustrates the distribution remaining after a 65% deep bleach. This postbleach distribution shows that the photobleaching selectivity is very subtle; e.g., for regions with correlation times differing by 1.2 orders of magnitude, the photobleaching efficiency in the slower regions is only 25% less than that in the faster regions.

Once α is determined, the initial anisotropy $r(0)$ of the whole ensemble can be calculated for various bleach depths (eq A7). The calculated functions exhibit the same trend as those observed in the experiment (see Figure 7).

(b) Relationship between True and Apparent Distributions. For the standard-photobleaching experiments, we have assumed that the measured correlation time τ_c can characterize the dynamics of the entire ensemble as long as the bleach depth is small enough, e.g., ≤ 0.1. To test this assumption, we calculated the "true" average correlation time, τ_{true}, directly from the distribution of rotational correlation times. The calculated average correlation times τ_{obs} at bleach depths 0.01 (defined as τ_c in the simulation) and 0.1 both differ from τ_{true} by less than 10%. As a result, within our experimental error of 10%, the correlation time τ_c obtained after a shallow bleach (bleach depth ≤ 0.1) reasonably represents the true average correlation time of the entire ensemble even with a biased photobleaching efficiency.

Furthermore, the KWW β parameter of the distribution following a shallow bleach (bleach depth 0.1) is calculated to be 0.59, consistent with the value of 0.6 for the initial equilibrium distribution. Hence, this result verifies the assump-

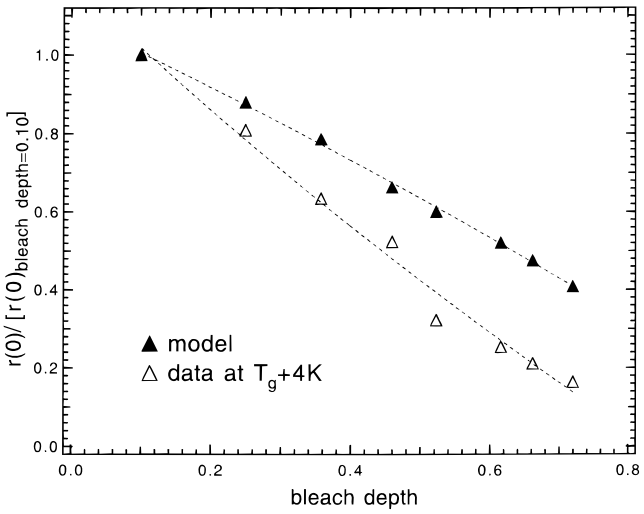

Figure 7. Initial anisotropy $r(0)$ obtained from the experiments (open triangle) and the simulation (solid triangle) as a function of bleach depth for tetracene in OTP at $T_g + 4$ K. These values are normalized to those observed for a bleach depth of 0.10.

tion that, for very small bleach depths (≤ 0.1), the observed postbleach distribution is not significantly different from the true distribution of relaxation times. The model also makes predictions for the dependence of β upon bleach depth and for the β value observed in a shallow-bleaching experiment after a deep bleach. These predictions are compared to experiment in Table 1. The model agrees with experiment in that β values near 0.6 are consistently observed.

(c) Interpretation of Deep-Bleaching Experiments. For the measurements of the time evolution of $\tau_{obs}(\Delta t)$, it is impossible to perform a shallow bleach immediately after a 65% deep bleach and acquire the average correlation time at short waiting times ($\tau_{obs}(\Delta t \approx 0)$). Instead, we used the average correlation time obtained from the anisotropy decay after a linearly polarized 65% deep bleach (τ_{obs}) as the first data point in Figure 4, $\tau_{obs}(\Delta t = 0)$. However, we were able to calculate $\tau_{obs}(\Delta t = 0)$ in the simulation. The correlation time $\tau_{obs}(\Delta t = 0)$ was calculated with a 0.1 bleach depth for a normalized distribution of relaxation times, which represents the remaining population following a 65% deep bleach. The correlation time τ_{obs} for a 0.65 bleach depth was calculated from the original equilibrium distribution. The results show that these two numbers are only 7% different. It is notable that a 7% error in the $\Delta t = 0$ point in Figure 4 does not affect the exponential fit enough to significantly change the integrated exchange time.

V. Concluding Remarks

Using photobleaching techniques, we were able to selectively photobleach probe molecules in more mobile environments and observe a longer rotational correlation time for tetracene in supercooled *o*-terphenyl (OTP) near T_g. This observation supports the idea that spatially heterogeneous dynamics play an important role near T_g. In addition, after selectively photobleaching those probes with faster dynamics, we can measure the time required for the remaining slower-than-average probes to be redistributed into an equilibrium set of environments. At $T_g + 4$ K ($T_g = 243$ K), this exchange time is 6.5 times greater than the average probe rotational correlation time, τ_c, whereas Cicerone and Ediger reported an exchange time of $540\tau_c$ at $T_g + 1$ K in previous work.[4] Considering the experimental temperature range, these results are consistent with multidimensional NMR measurements for deuterated OTP[2] and suggest that there is a new relaxation process in supercooled liquids emerging only at temperatures very near T_g. This new relaxation process is suggestive of an underlying thermodynamic singularity such as the ones assumed in many theories of the glass transition.

Our new results are consistent with much but not all of the existing literature on exchange times in supercooled liquids near T_g. It may be that the emergence of a new relaxation process is not a universal phenomenon or that it happens in a somewhat different temperature range relative to T_g in different materials. We are currently performing similar photobleaching experiments on polystyrene.

Acknowledgment. This work was supported by the National Science Foundation (Grant CHE-9618824). We wish to thank Maurice Leutenegger for the investigation of the tetracene absorption spectrum in *o*-terphenyl at temperatures near T_g.

Appendix

In this section, we show how to calculate the bleach depth on the basis of the model described in section IVA, which assumes a distribution of relaxation times, $g(\tau)$, and a photobleaching efficiency function, $\Phi(\tau) \propto 1/\tau^{\alpha}$. Also shown is the calculation of the average correlation time τ_{obs} and the initial anisotropy $r(0)$ after a bleach. Calculations are first performed for a homogeneous environment and then averaged to produce the results for a heterogeneous system.

A. Relaxation within a Homogeneous Environment. It is assumed in this model that the relaxation is exponential in each region. That is, probe molecules within one region have the same rotational correlation time τ.

For a first-order photoreaction during the bleaching period, the change in concentration of probes with an absorption dipole moment at angle θ relative to the polarization of the bleaching beam is:

$$dc(\theta)/dt = -a(\cos^2\theta)\, c(\theta) \qquad \text{(A1)}$$

The variable a depends on the absorption strength, the light intensity, and the photobleaching yield, which is a function of probe relaxation time τ; i.e., $a = k\Phi(\tau)$. The photobleaching efficiency function $\Phi(\tau)$ is chosen as a power law, $1/\tau^{\alpha}$. The value of α was iterated to fit the experimental results and determines the photobleaching selectivity (see sections IVA and IVB). For a given α, the parameter k was varied to obtain different bleach depths.

The difference between the fluorescence intensities immediately before and after a bleach can then be written as

$$\Delta I_{\parallel} = 2\pi b\left[\frac{2}{3} + \frac{e^{-a}}{a} - \frac{1}{2a}\sqrt{\frac{\pi}{a}}\,\mathrm{erf}(\sqrt{a})\right] \qquad \text{(A2)}$$

$$\Delta I_{\perp} = 2\pi b\left[\frac{2}{3} + \frac{e^{-a}}{2a} - \left(\frac{1}{4a} - \frac{1}{2}\right)\sqrt{\frac{\pi}{a}}\,\mathrm{erf}(\sqrt{a})\right] \qquad \text{(A3)}$$

Parallel and perpendicular designations refer to the polarization of the reading beam relative to the bleaching beam. The constant b is a function of the initial probe concentration, the light intensity of the reading beam, and the probe fluorescence quantum yield; b includes factors not related to the probe relaxation time. The bleach depth of molecules with rotation time τ (bd_i) is calculated as follows:

$$\mathrm{bd}_i \equiv \frac{(2\Delta I_\perp + \Delta I_\parallel)/3}{I_0} = 1 - \frac{1}{2}\sqrt{\frac{\pi}{a}}\,\mathrm{erf}(\sqrt{a}) \qquad \text{(A4)}$$

I_0 is the fluorescence intensity before the bleaching. The initial anisotropy $r(0)_i$ can be calculated on the basis of the definition

$$r(0)_i \equiv \frac{\Delta I_\parallel - \Delta I_\perp}{\Delta I_\parallel + 2\Delta I_\perp} \qquad \text{(A5)}$$

B. Heterogeneous Environment. The entire ensemble consists of a distribution of homogeneous regions whose relaxation times are significantly different. As a result, the bleach depth for the whole ensemble is the weighted sum of the bleach depths from homogeneous regions with different correlation times:

$$\text{bleach depth} = \frac{\sum_i g_i(\mathrm{bd}_i)}{\sum_i g_i} \qquad \text{(A6)}$$

where g_i is the probability of finding probe molecules in regions with a correlation time τ and is obtained from the KWW distribution of relaxation times. The initial anisotropy of the entire ensemble is also calculated from the $r(0)_i$ from regions of different dynamics:

$$r(0) = \frac{\sum_i g_i(r(0)_i)}{\sum_i g_i} \qquad \text{(A7)}$$

Finally, the ensemble-averaged correlation time τ_{obs} can be calculated as follows:

$$\tau_{\mathrm{obs}} = \frac{1}{r(0)}\left[\frac{\sum_i g_i\,\mathrm{bd}_i\,r(0)_i\,\tau_i}{\sum_i g_i\,\mathrm{bd}_i}\right] \qquad \text{(A8)}$$

C. Consideration of Probe Reorientation during the Photobleaching Period. As discussed in section IVA, for subsets of probes with relaxation times faster than the bleaching time, it is not appropriate to assume that these probes maintain their orientation during the bleaching. Therefore, two refinements are added to the above calculation. First, $r(0)_i$ is assumed to be zero for these regions. Second, bleach depth in these regions is calculated using the following equation instead of eq A4:

$$\mathrm{bd}_i = 1 - \mathrm{e}^{-a/3} \qquad \text{(A9)}$$

Equation A9 is obtained by starting with the following replacement for eq A1:

$$\mathrm{dc}/\mathrm{d}t = -a\langle\cos^2\theta\rangle c \qquad \text{(A10)}$$

This treatment is approximate since we consider probe molecules to be either rapidly rotating or rigidly fixed during the bleaching pulse. Although in reality there are probes with intermediate dynamics, this population can be ignored if the distribution of relaxation times is sufficiently broad.

References and Notes

(1) Ediger, M. D.; Angell, C. A.; Nagel, S. R. *J. Phys. Chem.* **1996**, *100*, 13200.

(2) Bohmer, R.; Hinze, G.; Diezemann, G.; Geil, B.; Sillescu, H. *Europhys. Lett.* **1996**, *36*, 55.

(3) Schiener, B.; Chamberlin, R. V.; Diezemann, G.; Bohmer, R. *J. Chem. Phys.* **1997**, *107*, 7746.

(4) Cicerone, M. T.; Ediger, M. D. *J. Chem. Phys.* **1995**, *103*, 5684.

(5) Richert, R. *J. Phys. Chem. B* **1997**, *101*, 6323.

(6) Russell, E. V.; Israeloff, N. E.; Walther, L. E.; Gomariz, H. A. *Phys. Rev. Lett.* **1998**, *81*, 1461.

(7) Vogel, M.; Rossler, E. *J. Phys. Chem. A* **1998**, *102*, 2102.

(8) Arbe, A.; Colmenero, J.; Monkenbusch, M.; Richter, D. *Phys. Rev. Lett.* **1998**, *81*, 590.

(9) Moynihan, C. T.; Schroeder, J. *J. Non-Cryst. Solids* **1993**, *160*, 52.

(10) Cicerone, M. T.; Blackburn F. R.; Ediger, M. D. *J. Chem. Phys.* **1995**, *102*, 471.

(11) Tracht, U.; Wilhelm, M.; Heuer, A.; Feng, H.; Schmidt-Rohr, K.; Spiess, H. W. *Phys. Rev. Lett.* **1998**, *81*, 2727.

(12) Cicerone, M. T.; Blackburn, F. R.; Ediger, M. D. *Macromolecules* **1995**, *28*, 8224.

(13) Schmidt-Rohr, K.; Spiess, H. W. *Phys. Rev. Lett.* **1991**, *66*, 3020.

(14) Heuer, A.; Wilhelm, M.; Zimmermann, H.; Spiess, H. W. *Phys. Rev. Lett.* **1995**, *75*, 2851.

(15) Kuebler, S. C.; Heuer, A.; Spiess, H. W. *Phys. Rev. E* **1997**, *56*, 741.

(16) Cicerone, M. T.; Ediger, M. D. *J. Phys. Chem.* **1993**, *97*, 10489.

(17) Stevens, B.; Algar, B. E. *J. Phys. Chem.* **1968**, *72*, 3794.

(18) Heuer, A. *Phys. Rev. E* **1997**, *56*, 730.

(19) Gibbs, J. H.; DiMarzio, E. A. *J. Chem. Phys.* **1958**, *28*, 373.

(20) Adam, G.; Gibbs, J. H. *J. Chem. Phys.* **1965**, *43*, 139.

(21) Edwards, S. F.; Vilgis, Th. *Phys. Scr.* **1986**, *T13*, 7.

(22) Binder, K.; Young, A. P. *Rev. Mod. Phys.* **1986**, *58*, 801.

(23) Shlesinger, M. F.; Montroll, E. W. *Proc. Natl. Acad. Sci. U.S.A.* **1984**, *81*, 1280. Bendler, J. T.; Shlesinger, M. F. *J. Stat. Phys.* **1988**, *53*, 531.

(24) Kirkpatrick, T. R.; Thirumalai, D.; Wolynes, P. G. *Phys. Rev. A* **1989**, *40*, 1045. Kirkpatrick, T. R.; Thirumalai, D. *Transp. Theory Stat. Phys.* **1995**, *24*, 927.

(25) Miller, R. S.; MacPhail, R. A. *J. Chem. Phys.* **1997**, *106*, 3393.

(26) Perera, D.; Harrowell, P. *J. Non-Cryst. Solids*, in press.

(27) Kob, W.; Donati, C.; Plimpton, S. J.; Glotzer, S. C.; Poole, P. H. *Phys. Rev. Lett.* **1997**, *79*, 2827. Donati, C.; Douglas, J. F.; Kob, W.; Plimpton, S. J.; Poole, P. H.; Glotzer, S. C. *Phys. Rev. Lett.*, in press.

(28) Doliwa, B.; Heuer, A. *Phys. Rev. Lett.* **1998**, *80*, 4915.

(29) Heuer, A.; Tracht U.; Spiess, H. W. *J. Chem. Phys.* **1997**, *107*, 3813.

(30) Barkatt, A.; Angell, C. A. *J. Chem. Phys.* **1979**, *70*, 901.

(31) Fournie, G.; Dupuy, F.; Martinaud, M.; Nouchi G.; Turlet, J. M. *Chem. Phys. Lett.* **1972**, *16*, 332.

(32) As discussed in ref 16, these aging times are influenced by the sample cell and do not represent a time scale intrinsic to the material.

(33) The value of β was obtained from the KWW fit for tetracene reorientation in OTP near T_g.

(34) The KWW distribution function is calculated using Mathamatica by following the work of: Lindsey, C. P.; Patterson, G. D. *J. Chem. Phys.* **1980**, *73*, 3348.